

Recent progress in bidirectional interrogation techniques for enhancing multiplexing capability of fiber optic white light interferometric sensors

Libo Yuan, Limin Zhou, and Wei Jin

Citation: *Rev. Sci. Instrum.* **74**, 4893 (2003); doi: 10.1063/1.1614434

View online: <http://dx.doi.org/10.1063/1.1614434>

View Table of Contents: <http://rsi.aip.org/resource/1/RSINAK/v74/i11>

Published by the [American Institute of Physics](#).

Related Articles

High-resolution single-mode fiber-optic distributed Raman sensor for absolute temperature measurement using superconducting nanowire single-photon detectors

Appl. Phys. Lett. **99**, 201110 (2011)

Research on the fiber Bragg grating sensor for the shock stress measurement

Rev. Sci. Instrum. **82**, 103109 (2011)

Photonic crystal fiber injected with Fe₃O₄ nanofluid for magnetic field detection

Appl. Phys. Lett. **99**, 161101 (2011)

Highly efficient excitation and detection of whispering gallery modes in a dye-doped microsphere using a microstructured optical fiber

Appl. Phys. Lett. **99**, 141111 (2011)

A tilt sensor with a compact dimension based on a long-period fiber grating

Rev. Sci. Instrum. **82**, 093106 (2011)

Additional information on *Rev. Sci. Instrum.*

Journal Homepage: <http://rsi.aip.org>

Journal Information: http://rsi.aip.org/about/about_the_journal

Top downloads: http://rsi.aip.org/features/most_downloaded

Information for Authors: <http://rsi.aip.org/authors>

ADVERTISEMENT



**FIND THE NEEDLE IN THE
HIRING HAYSTACK**

Post jobs and reach
thousands of hard-to-find
scientists with specific skills



<http://careers.physicstoday.org/post.cfm> **physicstoday** JOBS

Recent progress in bidirectional interrogation techniques for enhancing multiplexing capability of fiber optic white light interferometric sensors

Libo Yuan^{a)}

Department of Physics, Harbin Engineering University, Harbin 150001, China

Limin Zhou

Department of Mechanical Engineering, The Hong Kong Polytechnic University, Hong Kong

Wei Jin

Department of Electrical Engineering, The Hong Kong Polytechnic University, Hong Kong

(Received 9 August 2002; accepted 29 July 2003)

In smart structure applications where fiber sensors are embedded within structural materials, multiple lead in/out fibers are preferred for redundancy and improving reliability. The use of only one lead/out fiber is not optimal because the breakage of a fiber at one location due to, for example, local structural damage, would cause the failure of the whole sensing system. The multiplexing and networking techniques suitable for such applications have attracted considerable research recently. In this article, based on the bidirectional interrogation technique for white light interferometric sensors arrays, a multiplexed fiber optic deformation sensor loop network suitable for smart structure applications has been designed and demonstrated. Loop-network sensor systems are based on the white light interferometric technique. Michelson and Mach–Zehnder optical path interrogators have been developed and demonstrated, respectively. For the usually used one direction interrogate sensing system, it is clear that multiplexed sensor arrays suffer from relatively large fiber segment-induced optical reflective and excess insertion loss that generally limit the total number of sensors that can be accommodated in this configuration. This loop-network bidirectional interrogating technique greatly extended the multiplexing capacity of fiber optic white light interferometric sensors system. A practical implementation of this technique is presented which makes use of a popular light emitting diode, superluminescent diode, or amplified spontaneous emission optical light source and standard single mode fiber, which are commonly used in the communication industry. The sensor loop topology is completely passive and absolute length measurements can be obtained for each sensing fiber segment so that it can be used to measure quasidistribution strain or temperature. For large-scale smart structures, this technique not only extends the multiplexing potential, but also provides a redundancy for the sensing system. It means that the sensor loop permits one point breakdown, because the sensing system will still work whenever the embedded sensor loop breaks somewhere. © 2003 American Institute of Physics. [DOI: 10.1063/1.1614434]

I. INTRODUCTION

In most distributed fiber optic sensing systems, sensors are fabricated or connected in one fiber line. Examples of these systems are fiber Bragg grating sensors,^{1,2} optical time domain reflectometer (OTDR) distributed sensors,^{3,4} white light distributed fiber optic sensing systems in parallel and in series types, etc.^{5–7} (They have one common drawback; if one sensor or somewhere in the fiber line, which embedded in the smart structure is broken.) The perceived requirement for optical sensor networks, rather than independent measuring devices, has stimulated the investigation of multiplexing and networking techniques for fiber point sensors.^{8,9}

White light interferometry, as a technique employing low coherence broadband light sources, has been a very active area of research in recently years. The idea of using a

short coherence length source to separate the signals returning from a series of sensors was first published by Al-Chalabi *et al.*,¹⁰ Brooks *et al.* proposed a series of Mach–Zehnder interferometers and ladder coherence multiplexing schemes.¹¹ Gusmeroli reported a low coherence polarimetric sensors array multiplexed on the fiber line.¹² Sorin *et al.*¹³ and Inaudi *et al.*¹⁴ further developed and simplified the quasidistributed low coherence fiber optic sensor array based on the Michelson interferometer.

Comparing the several distributed fiber sensing systems, such as the fiber Bragg grating (FBG) or in-line Fabry–Pérot sensing system, the simple and gauge length flexible characteristics of white light fiber optic interferometric quasidistributed strain sensors are attractive. For inhomogeneous materials, such as concrete, fiber reinforced polymers, timber, etc., the microscopic strain field will vary significantly if measured on the scale of the inhomogeneity. For such mate-

^{a)}Electronic mail: lbyuan@vip.sina.com

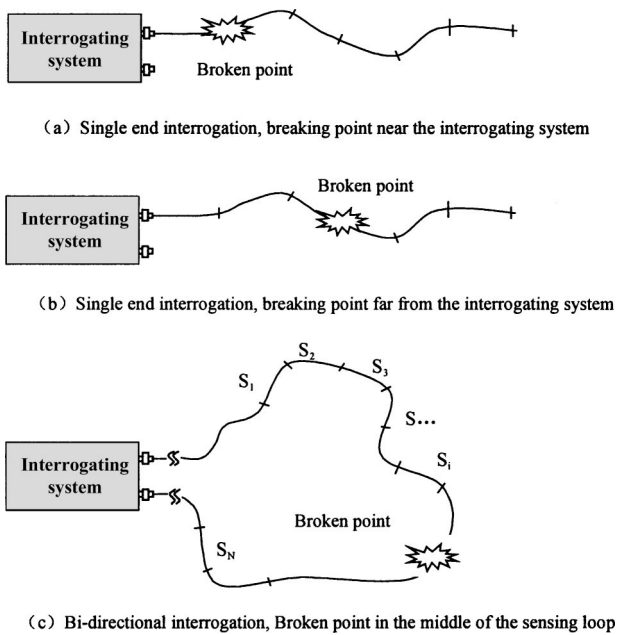


FIG. 1. Illustration of the fiber optic white light interferometric sensor network based on loop topology architecture. Most of sensors are still working even if some point is broken in the loop.

rials the sensor gauge length should be at least ten times the granularity of the material. In concrete the gauge length should probably be at least 100 mm, if macroscopic information is required. Strain sensors are best suited to monitor the local condition of the material and should be placed at the critical points of a structure where high strains are expected. While, for large structures, such as suspension bridges, that require dimensional stability, deformation measurements are important and gauge lengths for the sensors can be in the meters.

In this article, a white light interferometric fiber optic sensor ring network has been designed for distributed strain measurements in large-scale smart structures. The technique uses a scanning Mach-Zehnder interferometer or Michelson interferometer to interrogate the changes of optical path of fiber optic sensors from the bidirection of the optical fiber loop. The technique is capable of make absolute measurements with high resolution. The parameters that can be measured include strain and temperature. White light interferometers can be configured to perform quasidistributed measurement by multiplexing a number of sensors on to the fiber loop. The sensor ring network not only satisfies the redundancy requirement of a practical sensing system, but also provides a damage diagnosis methodology for large-scale smart structures.

II. PROBLEM STATEMENT

In many applications the sensor concept becomes increasingly viable if a network of sensors can be implemented using a single fiber optic bus to link the sensors together. In such systems there are obvious economies in fiber optic interconnects. Additionally, the terminal electronics can be efficiently shared between a number of sensors. The benefits

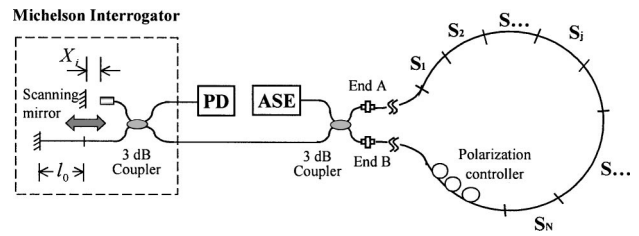


FIG. 2. Schematic of a multiplexed fiber optic loop sensor array with a Michelson interrogator.

thereby accrued lie not only in the capital cost of equipment but also in the more dominant sector involving installation costs.

The network topological requirements for each system is different, it varies depending upon the specific application. Perhaps the most important requirement is driven by the large-scale smart structures for multiple point or quasidistribution deformation, strain and temperature monitoring.

White light interferometry can be used as a passive coherence division multiplexing technique for interrogating an array of fiber optic sensors. However, for the case when all sensors are multiplexed on one fiber line and embedded within a large scale smart structure, a very critical issue is that if somewhere there is break due to the local damage or a crack in the structure, it will lead to part of the system not working or at the worst case, the whole system failure. This is illustrated in Figs. 1(a) and 1(b).

If a loop topology and a bidirectional interrogation technique, as shown in Fig. 1(c), were adopted, most of the sensors in the system would still function normally even if a particular sensor or failed sensor in the transmission fiber line was damaged. This is because the sensing information for each sensor is coherent twice from two fiber ends and improves system reliability.

III. BIDIRECTIONAL INTERROGATION TECHNIQUE BASED ON A LOOP TOPOLOGY

Like other coherence-multiplexed schemes, the bidirectional interrogation technique (BDIT) uses separate receiving interferometers whose time delays are matched to the remote sensing gauge reflective signals pair. It is classified by two types based on the Mach-Zehnder and Michelson interrogation architectures,^{15,16} as shown in Figs. 2 and 3. The common characteristic of this scheme is all sensors connected to

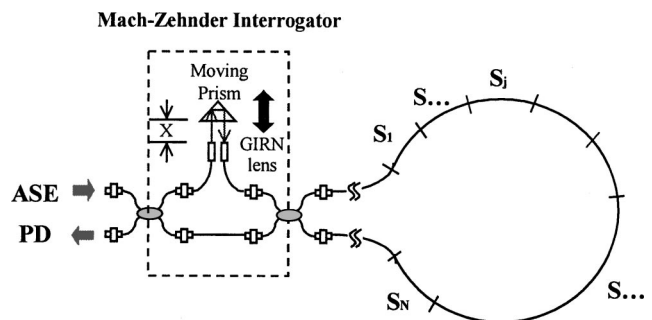


FIG. 3. Bidirection interrogator based a Mach-Zehnder fiber optic white light interferometer.

each other and linked, forming a fiber loop topology, which ensures that it can be interrogated by way of bidirection. One of the advantages of the BDIT is the enhanced multiplexing capacity. It provides double sensors unlike the one end array case. The looped sensors are completely passive and supply absolute length measurements for each fiber-sensing gauge. The proposed sensing scheme can be used to measure quasideistribution strain or temperature. For the large-scale smart structure, this technique not only extended the sensors number, but also provides a redundancy for the sensing system. It means that the sensor loop permits one point breakdown, because the sensing system will still work whenever the embedded sensor array breaks somewhere.

A. Michelson interrogation system

The extended-multiplexing low-coherence reflectometry loop sensor array using a Michelson interrogation is shown in Fig. 2. The light source is an erbium-doped fiber amplifier, which provided up to 10 mW of amplified spontaneous emission (ASE) at a wavelength of $1.55 \mu\text{m}$. The low-coherence light via a fiber optic isolator is launched into the Sagnac-like fiber loop by a fused 3 dB coupler. The fiber loop consists of N sections of a 1-m-length single-mode fiber connected in series, forming a loop N -sensor array. Reflected light from this fiber loop is coupled into an optical low-coherence reflectometer (OLCR). Inside the OLCR, the light signals split by a second 3 dB coupler. The lower (reference) path is reflected directly by the mirrored fiber end and then leads to the photodiode (PD) detector. The upper path leads to the fiber optic collimator and is reflected by a moving scanning mirror, then the signals are guided to the PD detector.

The reflectivities of the in-line reflectors in between the two sensing segments are very small, and equal to 1% or less to avoid depletion of the input probe signal. The fiber sensor lengths l_i between adjacent reflectors can be of any value as long as the differences in their lengths are not larger than the scan range of the OLCR. In our experiments, l_i has been chosen to be about 1 m long and the reference gauge lengths l_0 are nearly the same as the sensor length. The length differences between any two of the sensors are within 270 mm corresponding to the 400 mm scan range of the OLCR in free space. As the OLCR is scanned, the white light interference patterns occur whenever the path difference matches the distance between adjacent reflectors in the sensor loop.

B. Mach–Zehnder interrogation system

The loop network using a Mach–Zehnder interrogator is shown in Fig. 3. It consists of a light emitting diode (LED) or superluminescent diode (SLD) light source, a photodiode detector, a fiber optic Mach–Zehnder optical path interrogating part, and a number of fiber segments connected in series and forming a loop network. The light launched into the ring network-sensing array first passes the Mach–Zehnder interrogator and reaches the fiber optic sensor array. The optical-path difference (OPD) of the Mach–Zehnder interferometer can be varied through the use of a scanning prism. The scanning prism is used to adjust the OPD of the Mach–Zehnder

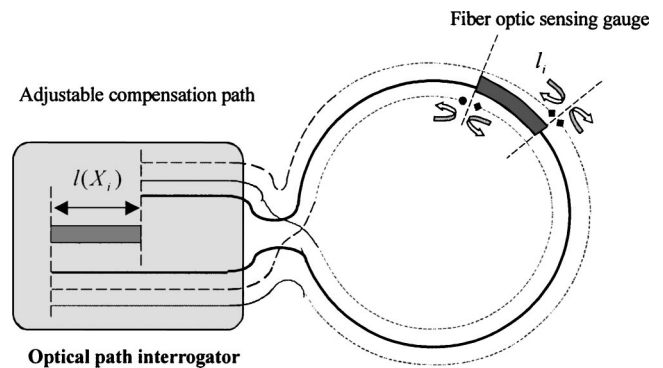


FIG. 4. Working principle of the bidirection optical path interrogator adjusting the compensation path to match each sensor gauge.

interferometer to match and trace the change of the fiber length in each sensing segment. We make the OPD of the Mach–Zehnder interferometer nearly equal to the fiber sensor gauge length, so that the two reflected lightwaves from the two-end surfaces of each sensing gauge can match each other. When the OPD of the Mach–Zehnder interferometer is equal to the gauge length of a particular sensor, a white light fringe pattern is produced. (Similar to the case of the Michelson interrogator, the interference central fringe, which is located in the center of the fringe pattern and has the highest amplitude peak, corresponds to the exact match of the OPD for the sensor.) As the optical path of the fiber sensor is modulated by the ambient perturbation, for instance, strain or temperature, then the perturbation parameters related to the optical path change will be measured and recorded by the shift of the interference signal peak.

C. Discussions

For the two sensor schemes mentioned above, if under the condition of same light power, comparing the intensity of the sensor output signal, the Mach–Zehnder scheme is larger than the Michelson scheme, that means when the light source power is lower, the Mach–Zehnder scheme is preferable in order to enhance the sensor multiplexing capability. When the light source power is big enough, Michelson scheme is preferable, because the one-directional collimator-mirror system is easy to install and adjust for the practical system.

IV. PRINCIPLE OF OPERATION

The fundamental operation of this bidirection optical path interrogation approach is based on optical fiber white light interferometry. As shown in Fig. 4, it consists of two parts linked by a 3 dB coupler, one part is the fiber loop with N fiber optic segments connected to each other to form an N sensor array, and the other part is the Michelson or Mach–Zehnder-type optical path interrogator. We assume that the i th fiber optic sensor gauge length is l_i in the sensor array loop. The optical signals are reflected from two ends of the fiber optic sensor i . The sensing optical path difference (SOPD) of these two reflective optical signals is nl_i , while the variable compensation path can be adjusted by a scanning mirror (or a prism), which is mounted on a moving translation stage, as shown in Fig. 2 (or Fig. 3 in the case of

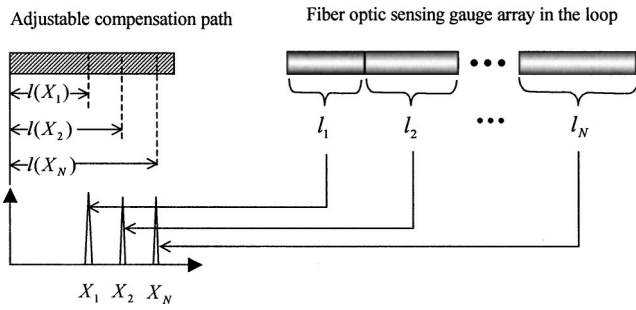


FIG. 5. N unique output optical signals corresponding to each fiber optic sensor gauge in the sensing loop.

a moving prism). The gauge lengths of the sensors (l_1, l_2, \dots, l_N) are chosen to be slightly different from one another and approximately the same as the sensing optical path-length difference. It can be tuned through the use of a scanning mirror or prism system. When the mirror or prism is tuned to a position where the compensation optical path difference (COPD) of the interrogator is matched to the gauge length of a particular sensor, a white light interferometric pattern is generated. The highest amplitude fringe of the white light interference pattern located in the center of the fringe pattern corresponds to exactly the same matched optical path between the SOPD and COPD. If we adjust the variable compensation optical path difference in the Michelson or Mach-Zehnder interrogator to match the SOPD, then by way of tracing and recording the change of COPD $l(X_i)$, the variation of the SOPD can be measured via the measurement of the displacement of the compensation optical path, which corresponds to the change of the fiber optic sensor gauge variation, as shown in Fig. 5. The optical signals reflected from the two ends of the sensor not only come from the clockwise direction, as the solid line illustrates in Fig. 4, but also come from the counterclockwise direction, as the dotted line shows in Fig. 4, due to the symmetry of the fiber loop topology. This is why we call it a “bidirectional” interrogating system.

Therefore, the deformation of sensor i can be measured by tracing the change of the mirror moved displacement ΔX_i :

$$\Delta X_i = \Delta(nl_i), \tag{1}$$

where n is the refractive index of the fiber guide mode. Thus, it can be used as a powerful tool to measure quasidistribution strain or temperature by the following relationship:

$$\varepsilon_i = \frac{\Delta X_i}{n_{\text{equivalent}} l_i} \tag{2}$$

and

$$(T_i - T_{0i}) = \frac{\Delta X_i}{l_i(T_{0i})n(\lambda, T_{0i})[\alpha_f + C_T]}, \tag{3}$$

where $n_{\text{equivalent}} = n\{1 - (1/2)n^2[(1 - \nu)p_{12} - \mu p_{11}]\}$ represents the equivalent refractive index of the fiber guide mode. For silica materials at wavelength $\lambda = 1550$ nm, the parameters are $n = 1.46$, Poisson ratio $\nu = 0.17$, and photoelastic constants $p_{11} = 0.12$ and $p_{12} = 0.27$, taken from Ref. 17. $n(\lambda, T_{0i})$ is the refractive index of the optical fiber under the condition of wavelength λ and i th sensor ambient temperature T_{0i} . Here, α_f and C_T are the thermal expansion coefficient and the refractive index temperature coefficient of the optical fiber, respectively. $\alpha_f = 5.5 \times 10^{-7}/^\circ\text{C}$, $C_T = 0.811 \times 10^{-5}/^\circ\text{C}$ at wavelength $\lambda = 1550$ nm are taken from Ref. 18.

V. MULTIPLEXING CAPACITY

As the scanning mirror moves on the translation stage, there will be N groups of interference fringe patterns appearing which corresponds to the OPD of the interferometer matched to that of the N sensors in the loop. The peak fringe intensity at the photodetector corresponds to the i th sensor, which is due to the coherent mixing between the reflected waves from the i th and the $(i + 1)$ th reflectors, and may be expressed as

$$I_D(i) = \frac{I_0}{16} \sqrt{R_f R_m \eta(X_i)} \left\{ \begin{aligned} & \left[\prod_{k=1}^{i-1} T_k \beta_k \right] \left[\prod_{k=1}^{i-1} T'_k \beta'_k \right] \sqrt{R_i R_{i+1} T_i \beta_i T'_i \beta'_i} \\ & + \left[\prod_{k=i+2}^{N+1} T'_k \beta'_k \right] \left[\prod_{k=i+2}^{N+1} T_k \beta_k \right] \sqrt{R'_i R'_{i+1} T'_{i+1} \beta'_{i+1} T_{i+1} \beta_{i+1}} \end{aligned} \right\}, \tag{4}$$

where I_0 represents the light intensity coupled into the input optical fiber from the ASE source. The insertion loss of the 3 dB coupler has been neglected. β_i and β'_i represent, respectively, the excess losses associated with sensor S_i , which is due to the connection loss between the sensing segments, for the cw and the ccw propagating lightwaves. $T_i(T'_i)$ and $R_i(R'_i)$ are, respectively, the transmission and reflection coefficients of the i th partial reflector. $T_i(T'_i)$ is in general

smaller than $1 - R_i$ ($1 - R'_i$) because of the loss factor $\beta_i(\beta'_i)$. The values of T_i , R_i , and β_i could be different from that of T'_i , R'_i , and β'_i . $\eta(X_i)$ is the loss associated with the scanning mirror and collimating optics and is a function of the scanning mirror position $X_{i,i+1}$. R_f and R_m are the reflectivities of the mirrored fiber end and the scanning mirror, respectively.

In the fiber optic sensor loop array, the fraction of optical

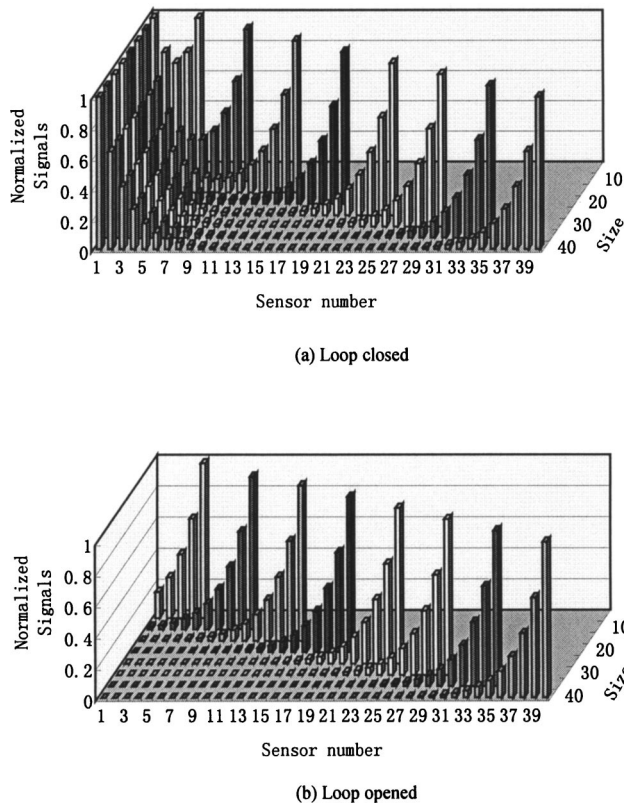


FIG. 6. Normalized output signal intensities for different fiber sensors loop size.

source power is coupled into the fiber and distributed over the sensor array via several connectors. Each sensor element absorbs or diverts a certain amount of power (insertion loss), typically, between 0.1 and 0.5 dB. If the minimum-detecting limit of the photodiode is I_{min} , then the maximum number of the total fiber optic sensors can be evaluated by the condition

$$I_D(i) \geq I_{min}. \tag{5}$$

For convenience in calculating, we neglect the excess insertion loss of the two 3 dB coupler and assumed that the typical fiber optic connection insertion loss coefficient $\beta_i = \beta'_i = 0.9 (i = 0, 1, 2, \dots, N)$. Under the condition of perpendicular incidence, the reflectivity at the fiber end surface is given by Fresnel formula $R = (n - 1)^2 / (n + 1)^2$ where n is the index of the fiber core, and the typical value is 1.46, corresponding to 4% reflectivity. For good butt-connected fiber ends, the air gap is smaller than one wavelength, in that case the typically reflectivity $R_i (= R'_i)$ is nearly equal to 1%. Therefore, the transmission coefficient can be calculated as $T_i = T'_i = 0.89$. We assume that the average attenuation of the moving mirror part is 6 dB, i.e., $\eta(X_i) = 1/4$. Then, the normalized optical signal intensity versus the fiber optic sensor number i is plotted in Fig. 6(a) for different size sensor loop arrays. Compared with the open loop case, the sensor multiplexing capability is extended as twice as before, as shown in Fig. 6(b).

VI. PERFORMANCE OF THE SENSING SYSTEM

If in the case of two break points or more happened in the fiber sensor loop, the sensors between the first broken point and the last one will fail. It is different from the case of

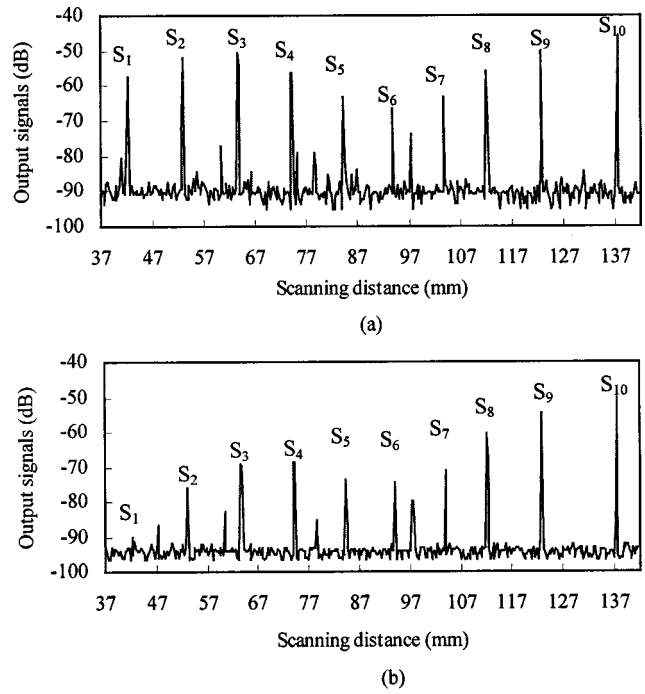


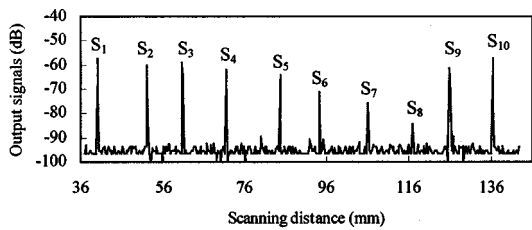
FIG. 7. Output from the ten fiber optic sensor array with input light source power = 0.47 dBm.

when just one break point occurs in the fiber loop. Generally, if just one point is broken in the fiber loop, the intensity of each sensor’s output signal will be decreased because, in that case, each sensor output signal is only supplied by one of two branches. When the light power is lower than the minimum requirements, the signals of the sensors far from the interrogator ports will emerge in the noise floor. The limitation case is that the break point is closed to port A or B.

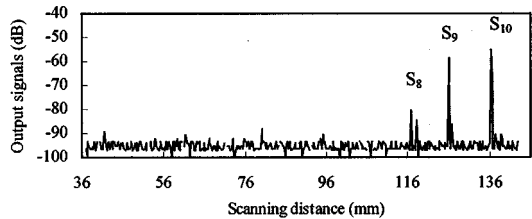
Figures 2 and 3 show the experimental arrangement used to demonstrate the looped fiber optic white light interferometric sensor array. An ASE light source was used in our experiment. The unpolarized light power of the ASE source is adjustable in the range of 0–10 mW. Ten optical fiber segments were connected to each other and used as fiber optic sensors. The fiber optic sensor gauge length was chosen to be nearly 1 m. The difference of each sensor gauge length is about 7 mm, and connected to each other by butt connectors. The ten sensor array output signal intensities are given in Fig. 7 for both cases of loop closed and loop open at end A, respectively.

It can be seen that the results shown in Figs. 7(a) and 7(b) essentially provide the same measurement information in terms of the positions of the peaks. This means that the system would function the same even if one end of the loop is opened. The signal level for the loop-closed case is, however, higher than the loop-open case.

For the particular light level of 0.47 dBm, the signal level for sensor S_1 is obviously small for the peak position when the loop is open at end A [Fig. 7(b)], similarly, it is open at end B due to the symmetry of the loop architecture. The signal level was significantly enhanced when the loop was closed [Fig. 7(a)]. This means that, for the same source power level, the maximum sensor number can be increased with the closed-loop configuration.



(a) The output signals in case of loop open between 7-th and 8-th fiber optic sensor



(b) The output signals in case of fiber optic sensor array open between 7-th and 8-th sensor

FIG. 8. Redundancy of the bidirection interrogating fiber optic sensor loop topology.

The important characteristic for a fiber optic sensor system is its redundancy ability, especially in the case of embedded sensor chains into the structure. In order to test the redundancy performance of the bidirection interrogation fiber optic sensing system, the fiber optic loop disconnected experiment has been made in both cases of looped fiber sensor chains and the sensors linked in a linear array along a fiber line. The test results are plotted in Fig. 8. We have disconnected the sensor chain between 7th and 8th sensors for the all ten sensor chains. It can be seen that the output signals of sensors 1–7 vanish in the case of the ten-sensor array in one fiber line and interrogate from one port, as shown in Fig. 8(b). However, the ten sensors are still working when disconnected between the 7th and 8th sensor. The output signals, as shown in Fig. 8(a), would still be there except that the signal amplitude near the 8th sensor is lower than before.

It should be mentioned that, although the measurement results for a linear array with a loop open at either end A or B is polarization independent (in the strict sense, the effect of polarization is neglected in that case), the results obtained from the closed-loop measurements are under the influence of the polarization states. Figure 9 shows the variation of the signals when the polarization controller in the loop (see Fig. 2) was adjusted. This is because light signals that are not reflected at the partial reflectors (transmitted) would mix coherently at the loop coupler as they traveled through the optical path length. When the counterpropagating (transmitted) light signals are of the same polarization states, the light signal at the output port of the loop would approach zero due to destructive interference.¹⁹ When the counterpropagating signals are of different polarizations, the orthogonal polarization components would add up in intensity and result in a

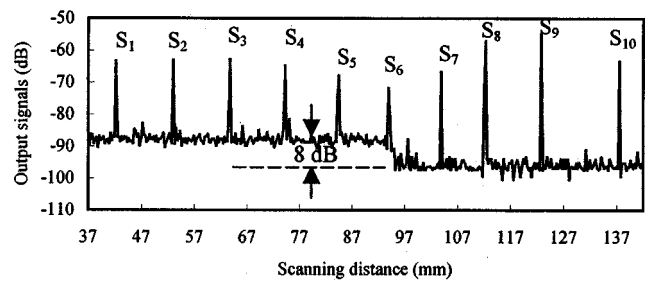


FIG. 9. On the condition of input light source power is 0.47 dBm, a 8 dB reduction in the noise floor is achieved by adjusting the polarization states.

noise floor. And, the variation of deformation in each gauge length of the sensor starting from the first sensor would change the state of polarization. In that case, their multisensing capability would have been reduced. It may, therefore, be necessary to control the polarization states in order to achieve the optimal results. One method is by way of inserting a depolarizer between the ASE light source and the 3 dB coupler, the other solution is using polarization to maintain the fiber in the sensing system to overcome the unstable polarization state.

ACKNOWLEDGMENTS

This work was supported by the National Natural Science Foundation of China, Grant No. 50179007, and the Teaching and Research Award Program for Outstanding Young Professors in Higher Education Institute, MOE, P.R.C., and the Science Foundation of Heilongjiang Province for Outstanding Youth, 1999, to the Harbin Engineering University.

- ¹A. D. Kersey and W. W. Morey, *Electron. Lett.* **29**, 112 (1993).
- ²G. Duck and M. M. Ohn, *Opt. Lett.* **25**, 90 (2000).
- ³E. Sensfelder, J. Burck, and H. J. Ache, *Appl. Spectrosc.* **52**, 1283 (1998).
- ⁴V. Lecoche, D. J. Webb, C. N. Pannell, and D. A. Jackson, *Opt. Commun.* **168**, 95 (1999).
- ⁵L. B. Yuan and Farhad Ansari, *Sens. Actuators A* **63**, 177 (1997).
- ⁶L. B. Yuan and L. Zhou, *Appl. Opt.* **37**, 4168 (1998).
- ⁷L. B. Yuan, L. Zhou, and W. Jin, *Opt. Lett.* **25**, 1074 (2000).
- ⁸J. M. Senior, S. E. Moss, and S. D. Cusworth, *Opt. Laser Technol.* **28**, 1 (1996).
- ⁹W. Ecke, I. Latka, R. Willsch, A. Reutlinger, and R. Graue, *Meas. Sci. Technol.* **12**, 974 (2001).
- ¹⁰S. A. Al-Chalabi, B. Culshaw, and D. E. N. Davies, *Proceedings of the 1st International Conference on Optical Fiber Sensors*, London (1983), pp. 132–135.
- ¹¹J. L. Brooks, R. H. Wentworth, R. C. Youngquist, M. Tur, B. Y. Kim, and H. J. Shaw, *J. Lightwave Technol.* **LT-3**, 1062 (1985).
- ¹²V. Gusmeroli, *J. Lightwave Technol.* **11**, 1681 (1993).
- ¹³W. V. Sorin and D. M. Baney, *IEEE Photonics Technol. Lett.* **7**, 917 (1995).
- ¹⁴D. Inaudi, S. Vurpillot, and S. Lloret, *Proc. SPIE* **2718**, 251 (1996).
- ¹⁵L. Yuan, L. Zhou, W. Jin, and J. Yang, *Opt. Lett.* **27**, 894 (2002).
- ¹⁶L. Yuan, W. Jin, L. Zhou, Y. H. Hoo, and S. M. Demokan, *IEEE Photonics Technol. Lett.* **14**, 1157 (2002).
- ¹⁷C. D. Butter and G. B. Hocker, *Appl. Opt.* **17**, 2867 (1978).
- ¹⁸L. B. Yuan, *Opt. Laser Technol.* **30**, 33 (1998).
- ¹⁹*Guided Wave Optical Sensors*, edited by W. Jin, Y. Liao, and Z. Zhang (Science, Beijing, China, 1998), pp. 148–176.